



# Measurement of $J/\psi$ decays into final states $2(\pi^+\pi^-)\pi^0$ , $K^+K^-\pi^+\pi^-\pi^0$ , $2(\pi^+\pi^-)$ and $K^+K^-\pi^+\pi^-$

V. V. Anashin<sup>1</sup>, O. V. Anchugov<sup>1</sup>, V. M. Aulchenko<sup>1,2</sup>, E. M. Baldin<sup>1,2</sup>, G. N. Baranov<sup>1,3</sup>, A. K. Barladyan<sup>1</sup>, A. Yu. Barnyakov<sup>1,3</sup>, M. Yu. Barnyakov<sup>1,2</sup>, S. E. Baru<sup>1,2</sup>, I. Yu. Basok<sup>1</sup>, A. M. Batrakov<sup>1</sup>, E. A. Bekhtenev<sup>1</sup>, A. E. Blinov<sup>1,2</sup>, V. E. Blinov<sup>1,2,3</sup>, A. V. Bobrov<sup>1,2</sup>, V. S. Bobrovnikov<sup>1,2</sup>, A. V. Bogomyagkov<sup>1,2</sup>, A. E. Bondar<sup>1,2</sup>, A. R. Buzykaev<sup>1,2</sup>, P. B. Cheblakov<sup>1</sup>, V. L. Dorohov<sup>1</sup>, S. I. Eidelman<sup>1,2</sup>, S. A. Glukhov<sup>1</sup>, D. N. Grigoriev<sup>1,2,3</sup>, V. V. Kaminskiy<sup>1</sup>, S. E. Karnaev<sup>1</sup>, G. V. Karpov<sup>1</sup>, S. V. Karpov<sup>1</sup>, K. Yu. Karukina<sup>1</sup>, D. P. Kashtankin<sup>1</sup>, A. A. Katsin<sup>1,2</sup>, T. A. Kharlamova<sup>1,2</sup>, V. A. Kiselev<sup>1</sup>, V. V. Kolmogorov<sup>1</sup>, S. A. Kononov<sup>1,2</sup>, K. Yu. Kotov<sup>1</sup>, A. A. Krasnov<sup>1</sup>, E. A. Kravchenko<sup>1,2</sup>, V. N. Kudryavtsev<sup>1</sup>, V. F. Kulikov<sup>1,2</sup>, E. A. Kuper<sup>1,2</sup>, G. Ya. Kurkin<sup>1,3</sup>, I. A. Kuyanov<sup>1</sup>, E. B. Levichev<sup>1,3</sup>, D. A. Maksimov<sup>1,2</sup>, V. M. Malyshev<sup>1,a</sup>, A. L. Maslennikov<sup>1,2</sup>, O. I. Meshkov<sup>1,2</sup>, S. I. Mishnev<sup>1</sup>, I. A. Morozov<sup>1</sup>, I. I. Morozov<sup>1,2</sup>, N. Yu. Muchnoi<sup>1,2</sup>, V. V. Neufeld<sup>1</sup>, S. A. Nikitin<sup>1</sup>, I. B. Nikolaev<sup>1,2</sup>, I. N. Okunev<sup>1</sup>, A. P. Onuchin<sup>1,2,3</sup>, S. B. Oreshkin<sup>1</sup>, A. A. Osipov<sup>1,2</sup>, I. V. Ovtin<sup>1,2</sup>, S. V. Peleganchuk<sup>1,2</sup>, V. V. Petrov<sup>1</sup>, P. A. Piminov<sup>1</sup>, S. G. Pivovarov<sup>1,3</sup>, V. G. Prisekin<sup>1,2</sup>, O. L. Rezanova<sup>1,2</sup>, A. A. Ruban<sup>1,2</sup>, V. K. Sandyrev<sup>1</sup>, G. A. Savinov<sup>1</sup>, A. G. Shamov<sup>1,2</sup>, D. N. Shatilov<sup>1</sup>, L. I. Shekhtman<sup>1</sup>, D. A. Shvedov<sup>1</sup>, B. A. Schwartz<sup>1,2</sup>, E. A. Simonov<sup>1</sup>, S. V. Sinyatkin<sup>1</sup>, A. N. Skrinsky<sup>1</sup>, A. V. Sokolov<sup>1,2</sup>, E. V. Starostina<sup>1,2</sup>, D. P. Sukhanov<sup>1</sup>, A. M. Sukharev<sup>1,2</sup>, A. A. Talyshev<sup>1,2</sup>, V. A. Tayursky<sup>1,2</sup>, V. I. Telnov<sup>1,2</sup>, Yu. A. Tikhonov<sup>1,2</sup>, K. Yu. Todyshev<sup>1,2</sup>, A. G. Tribendis<sup>1</sup>, G. M. Tumaikin<sup>1</sup>, Yu. V. Usov<sup>1</sup>, A. I. Vorobiov<sup>1</sup>, V. N. Zhilich<sup>1,2</sup>, A. A. Zhukov<sup>1</sup>, V. V. Zhulanov<sup>1,2</sup>, A. N. Zhuravlev<sup>1,2</sup>

<sup>1</sup> Budker Institute of Nuclear Physics, 11, akademika Lavrentieva prospect, Novosibirsk 630090, Russia

<sup>2</sup> Novosibirsk State University, 2, Pirogova street, Novosibirsk 630090, Russia

<sup>3</sup> Novosibirsk State Technical University, 20, Karl Marx prospect, Novosibirsk 630092, Russia

Received: 22 June 2022 / Accepted: 5 October 2022  
© The Author(s) 2022

**Abstract** Using the 1.32 pb<sup>-1</sup> statistics collected at the  $J/\psi$  peak with the KEDR detector at the VEPP-4M  $e^+e^-$  collider, we measured the branching fractions of  $J/\psi$  meson decays to the final states  $2(\pi^+\pi^-)\pi^0$ ,  $K^+K^-\pi^+\pi^-\pi^0$ ,  $2(\pi^+\pi^-)$  and  $K^+K^-\pi^+\pi^-$ . The results obtained for the decays  $J/\psi \rightarrow 2(\pi^+\pi^-)\pi^0$ ,  $J/\psi \rightarrow K^+K^-\pi^+\pi^-\pi^0$  contradict the measurements performed by other groups in the last century, but agree well with recent results of BABAR and BESIII collaborations.

## 1 Introduction

Among the known hadronic decays of the  $J/\psi$  meson, the decay  $J/\psi \rightarrow 2(\pi^+\pi^-)\pi^0$  has, according to the PDG data [1], the largest branching fraction,  $B(J/\psi \rightarrow 2(\pi^+\pi^-)\pi^0) = (3.73 \pm 0.32)\%$ . There are several measurements of the probability of this decay, performed in the 70s-80s of the

last century by groups MARKI ((4 ± 1)% [2]), PLUTO ((3.64 ± 0.52)% [3]), MARKII ((3.17 ± 0.42)% [4]) and DM2 ((3.25 ± 0.49)% [5]). In 2007 the BABAR collaboration, using the initial-state radiation, had measured the product  $\Gamma(J/\psi \rightarrow e^+e^-) \cdot B(J/\psi \rightarrow 2(\pi^+\pi^-)\pi^0)$ , having obtained the value  $303 \pm 5 \pm 18$  eV [6,7]. Dividing this value by  $\Gamma(J/\psi \rightarrow e^+e^-) = 5.53 \pm 0.10$  keV [1], we get from this result  $B(J/\psi \rightarrow 2(\pi^+\pi^-)\pi^0) = (5.48 \pm 0.35)\%$ , which is noticeably higher than values reported by groups [2–5]. In 2019 the BESIII collaboration performed a new measurement of this probability and obtained the value  $(4.73 \pm 0.44)\%$  [8], which agrees with the BABAR result, but poorly agrees with earlier measurements [3–5]. Recently, when studying the reaction  $e^+e^- \rightarrow 2(\pi^+\pi^-)\pi^0\pi^0\pi^0$ , the BABAR collaboration obtained for this branching fraction the result  $B(J/\psi \rightarrow 2(\pi^+\pi^-)\pi^0) = (3.47 \pm 0.61 \pm 0.52)\%$  [9]. This result is consistent with the PDG value [1], but has a worse accuracy compared to the previous measurement [6,7] and contradicts it.

In the same experiment [6,7] the BABAR collaboration also measured the product  $\Gamma(J/\psi \rightarrow e^+e^-) \cdot B(K^+K^-\pi^+\pi^-)$

S. I. Eidelman and A. P. Onuchin: Deceased.

<sup>a</sup> e-mail: [V.M.Malyshev@inp.nsk.su](mailto:V.M.Malyshev@inp.nsk.su) (corresponding author)

$\pi^-\pi^0$ ), having received the result  $107 \pm 4.3 \pm 6.4$  eV. Using this value, for the decay  $J/\psi \rightarrow K^+K^-\pi^+\pi^-\pi^0$  one can obtain the branching fraction  $B(J/\psi \rightarrow K^+K^-\pi^+\pi^-\pi^0) = (1.93 \pm 0.14)\%$ , which is in poor agreement with the PDG value  $B(J/\psi \rightarrow K^+K^-\pi^+\pi^-\pi^0) = (1.20 \pm 0.30)\%$ , based on a single measurement of this value, performed in 1977 by the MARKI group [10].

Thus, there is a clear contradiction between the results of measurements of these branching fractions, performed by various groups, which indicates the necessity for new measurements of these quantities. In this paper we present the results of measurements of the branching fractions  $B(J/\psi \rightarrow 2(\pi^+\pi^-)\pi^0)$  and  $B(J/\psi \rightarrow K^+K^-\pi^+\pi^-\pi^0)$ , performed with the KEDR detector. We also measured branching fractions of the  $J/\psi \rightarrow 2(\pi^+\pi^-)$ ,  $J/\psi \rightarrow K^+K^-\pi^+\pi^-$  decays and several  $J/\psi$  decays proceeding through intermediate hadronic resonances to the final states with four or five mesons.

## 2 KEDR data and event selection

The experiment was performed at the KEDR detector [11] of the VEPP-4M collider [12]. The analysis is based on data samples of  $(1.32 \pm 0.07) \text{ pb}^{-1}$  collected at the  $J/\psi$  peak, which corresponds to about 5.1 million  $J/\psi$  decays, as well as  $(82 \pm 4) \text{ nb}^{-1}$  collected at the energy lower than the  $J/\psi$  peak by 10 MeV for estimation non-resonant backgrounds. The luminosity is measured using single Bremsstrahlung online and small-angle Bhabha scattering offline.

At the first stage, the multihadron decays of the  $J/\psi$  meson were selected. The following criteria suppressing backgrounds from cosmic rays, beam-gas interactions and Bhabha events, were applied: total energy in the barrel liquid krypton (LKr) and endcap CsI calorimeters is greater than 0.8 GeV; at least four clusters with energies greater than 30 MeV in the calorimeters are reconstructed; at least one central track in the drift chamber (DC) is reconstructed.

At the second step candidates for the  $J/\psi \rightarrow X_i$  decays were selected, where  $X_i$  is  $2(\pi^+\pi^-)\pi^0$ ,  $K^+K^-\pi^+\pi^-\pi^0$ ,  $2(\pi^+\pi^-)$  or  $K^+K^-\pi^+\pi^-$  final state (hereinafter also denoted as  $5\pi$ ,  $2K3\pi$ ,  $4\pi$  and  $2K2\pi$  respectively). For this it was required that for a given decay channel the corresponding number of final  $\pi^\pm$ ,  $K^\pm$  and  $\pi^0$  be registered, while an arbitrary number of additional photons was allowed. The central tracks in the DC were identified as  $\pi^\pm$  or  $K^\pm$  for the track momentum  $P < 0.6$  GeV using the barrel part of the time-of-flight system of scintillation counters (ToF), and for  $P > 0.6$  GeV using a system of Cherenkov counters (ATC). A cluster in LKr or CsI calorimeter with energy  $E_{\text{cl}} > 50$  MeV was considered a photon if it was not associated with reconstructed tracks in drift chamber. For each photon in the event, all possible combinations with other photons were enumer-

ated. A combination of two photons with a mass closer to the mass of  $\pi^0$  than double the mass resolution was considered as a  $\pi^0$  candidate. Of the  $\pi^0$  candidates for a given photon, the combination with the mass closest to the  $\pi^0$  mass was considered to have originated from the decay of  $\pi^0$ .

For the selected candidate events, a 4C or 5C kinematic fit was made, assuming that the  $J/\psi \rightarrow X_i$  decay occurred. Constraints on the total energy, the components of the total momentum of the final particles and the mass of  $\pi^0$ , if is present in the final state, were imposed. An event was considered to be a signal if the condition  $\chi^2 < \chi^2_{\text{CUT}}$  for  $\chi^2$  of kinematic fit was satisfied, where  $\chi^2_{\text{CUT}}$  was taken equal to 50 for the decays  $J/\psi \rightarrow 5\pi$ ,  $J/\psi \rightarrow 2K3\pi$ , and equal to 40 for the  $J/\psi \rightarrow 4\pi$  and  $J/\psi \rightarrow 2K2\pi$  decays.

To determine the detection efficiency for signal events, the KEDRSIM simulation package, based on the GEANT3 code [13], was used, wherein the  $J/\psi \rightarrow X_i$  decays were modeled with a generator based on the helicity formalism [14, 15]. To estimate the contribution of background events, we used the LundCharm generator [16], based on the JETSET code [17] and adapted for charmonium decays. A final state radiation was taken into account with the help of the PHOTOS package [18].

## 3 Data analysis and estimation of systematic uncertainties

The branching fractions of the  $J/\psi \rightarrow X_i$  decays were determined with the formula

$$B_i = B_{mh} \frac{N_i^{\text{peak}} - N_i^{\text{cont}} \cdot L / L^{\text{cont}}}{N_{mh}^{\text{peak}} - N_{mh}^{\text{cont}} \cdot L / L^{\text{cont}}} \frac{\varepsilon_{mh}^{\text{MC}}}{\varepsilon_i^{\text{MC}}} \frac{R_i^{\text{MC}}}{R_i^{\text{exp}}}, \quad (1)$$

where  $B_i$  is the branching fraction of  $J/\psi \rightarrow X_i$  decay,  $B_{mh} = (87.7 \pm 0.5)\%$  [1] is the branching fraction of  $J/\psi$  multihadron decays.  $N_i^{\text{peak}}$  is the number of selected  $X_i$  signal events at the  $J/\psi$  peak after subtracting the background from decays other than  $J/\psi \rightarrow X_i$ ,  $N_i^{\text{cont}}$  is the number of selected  $X_i$  signal events out of peak.  $N_{mh}^{\text{peak}}$  and  $L$  are the number of selected multihadron events and the integrated luminosity at the  $J/\psi$  peak,  $N_{mh}^{\text{cont}}$  and  $L^{\text{cont}}$  are the same off-peak quantities, respectively. In the formula  $\varepsilon_{mh}^{\text{MC}} = 0.938$  and  $\varepsilon_i^{\text{MC}}$  are the Monte Carlo (MC) estimated detection efficiencies for  $J/\psi$  multihadron decays and decays  $J/\psi \rightarrow X_i$ .  $R_i^{\text{exp}}$  and  $R_i^{\text{MC}}$  are the fractions of signal events in candidate events for  $J/\psi \rightarrow X_i$  decays, for experimental data and MC simulation, respectively.

Figure 1 shows the  $\chi^2$  distributions of the kinematic fits for the selected events at the  $J/\psi$  peak, as well as the distributions for the selected events outside the resonance, scaled

by the ratio of the integrated luminosities at the peak and in the continuum. The experimental data were fitted using linear combinations of the distributions of signal and background decays of  $J/\psi$  obtained in the simulation, herewith the normalization factors for the distributions were considered as free parameters. The fitting range was chosen large enough so that, at large values of  $\chi^2$ , the contribution of signal events was much smaller compared to background events. Thus, the background value was actually determined from the “tail” of the distribution. It can be seen from the figure that, at small values of  $\chi^2$ , the distributions in the simulation and experiment are agree worse. For that reason, the number of signal events  $N_i^{peak}$  was determined not from the fit, but was calculated as the difference between the number of selected experimental events and the number of background events determined from the fit and satisfying the condition  $\chi^2 < \chi^2_{CUT}$ . However, due to the difference in  $\chi^2$  distributions, the fractions of signal events in the total number of selected  $J/\psi \rightarrow X_i$  decays can differ for experimental data and modeling, which leads to different efficiencies for signal events. To take these differences into account, corrections were introduced into formula (1) by means of  $R_i^{exp}/R_i^{MC}$  factors, which for decays  $J/\psi \rightarrow 5\pi$ ,  $J/\psi \rightarrow 2K3\pi$ ,  $J/\psi \rightarrow 4\pi$  and  $J/\psi \rightarrow 2K2\pi$  equal  $0.983 \pm 0.010$ ,  $1.046 \pm 0.041$ ,  $1.008 \pm 0.036$  and  $1.033 \pm 0.030$  correspondingly, where the given errors are mainly determined by the statistical errors of the experimental data.

Among the selected multihadron decays of  $J/\psi$ , there is a noticeable fraction of background events. Of these, about 40% are Bhabha events, approximately 10% are beam-gas interactions, about 50% are cosmic events, and there is also a small fraction ( $\approx 0.5\%$ ) of non-resonant continuum events. The fraction of these background events is estimated from the number of selected multihadron decays  $N_{mh}^{cont} = 32.3 \cdot 10^3$  for off-resonance data, taking into account the difference in integrated luminosities at the  $J/\psi$  peak and in the continuum, and is about 11%. In formula (1), these background events are subtracted from the number of selected multihadron decays  $N_{mh}^{peak} = 4.62 \cdot 10^6$ . The systematic error associated with such a subtraction is mainly determined by the luminosity measurement accuracy and does not exceed 1.6%. For Bhabha-scattering events, it is also necessary to take into account the possible interference with  $J/\psi \rightarrow e^+e^-$  decays when subtracting. However, because the data were collected at the maximum of the  $J/\psi$  production cross section, these interference effects are suppressed and can be neglected. Estimation of the contribution of cosmic events to  $N_{mh}^{peak}$ , strictly speaking, must be done in accordance with the time of collecting statistics. However, peak and continuum statistics, as a rule, were collected under the same conditions (initial beam currents, luminosities, data collection time per run), and the ratio of data acquisition times at the peak and in the continuum coincides with the  $L/L^{cont}$  ratio with a good

accuracy ( $\approx 4\%$ ). When selecting  $5\pi$ ,  $2K3\pi$ ,  $4\pi$ , and  $2K2\pi$  events for data out of resonance, due to more stringent selection conditions, the continuum events are mainly selected. Their numbers are small, systematic errors arising from their subtraction in formula (1) are mainly determined by possible interference between the amplitudes of  $J/\psi$  decays and continuum processes. They are evaluated below when considering the effects of interference.

The numbers of selected signal events  $N_i^{peak}$  and  $N_i^{cont}$ , the detection efficiencies  $\varepsilon_i$  with systematic uncertainties, the measured branching fractions  $B_i$  of the  $J/\psi \rightarrow X_i$  decays, as well as the PDG values for these quantities are shown in Table 1. The first of the given errors for the measured branching fraction is statistical and the second is systematic. The details of determining the efficiencies  $\varepsilon_i$  and their errors are given below. Estimates of systematic errors for the measured decay rates  $J/\psi \rightarrow X_i$  are shown in Table 2.

Systematic error due to possible difference in track registration efficiency for data and modeling was estimated as follows. The track registration efficiency was determined using  $J/\psi \rightarrow 2(\pi^+\pi^-)\pi^0$  decays. For selected multihadron events with three or four charged pions, one neutral pion and arbitrary number of additional photons, the distributions over square of the recoil mass of  $3\pi\pi^0$  system for data and simulation were considered (for  $4\pi\pi^0$  events, four possible combinations were taken). For each range of polar angle and absolute value of the recoil momentum the experimental distributions were fitted using linear combinations of MC histograms for the  $J/\psi \rightarrow 2(\pi^+\pi^-)\pi^0$  decays and other  $J/\psi$  decays considered as background. Then, after subtracting the backgrounds from the  $4\pi\pi^0$  and  $3\pi\pi^0$  distributions, the numbers  $N_4$  and  $N_3$  were determined when track from the  $J/\psi \rightarrow 2(\pi^+\pi^-)\pi^0$  decay was reconstructed or not, respectively. Track registration efficiency was calculated as  $\varepsilon_{tr}^{exp} = N_4/(N_4 + N_3)$ , and in the range of track polar angles  $60^\circ$ - $120^\circ$  and track momenta from 0.8 to 1.5 GeV/c it is about 96%. In the same way, track registration efficiency  $\varepsilon_{tr}^{MC}$  was determined for the  $J/\psi \rightarrow 2(\pi^+\pi^-)\pi^0$  decays in simulation. Then, when selecting events to determine the detection efficiency of  $J/\psi \rightarrow X_i$  decays, some fraction of selected events in the simulation was discarded in order to obtain equal track efficiencies  $\varepsilon_{tr}^{MC}$  and  $\varepsilon_{tr}^{exp}$ . The corrections to the measured branching fractions of the  $J/\psi \rightarrow 4\pi$  and  $J/\psi \rightarrow 2K2\pi$  decays due to this were 6.2% and 10.5%, respectively. The residual difference between the  $\varepsilon_{tr}^{MC}$  and  $\varepsilon_{tr}^{exp}$  efficiencies after that for all ranges of the track momenta does not exceed 0.9%, which gives for the measured  $J/\psi$  decays branching fractions an upper estimate of 3.6% for the systematic uncertainty associated with the track detection efficiency, as shown in Table 2.

The  $\pi^0$  registration efficiency was determined in a similar way, also using the  $J/\psi \rightarrow 2(\pi^+\pi^-)\pi^0$  decays. In the multihadron decays of  $J/\psi$  the events  $2(\pi^+\pi^-)\pi^0$  as well

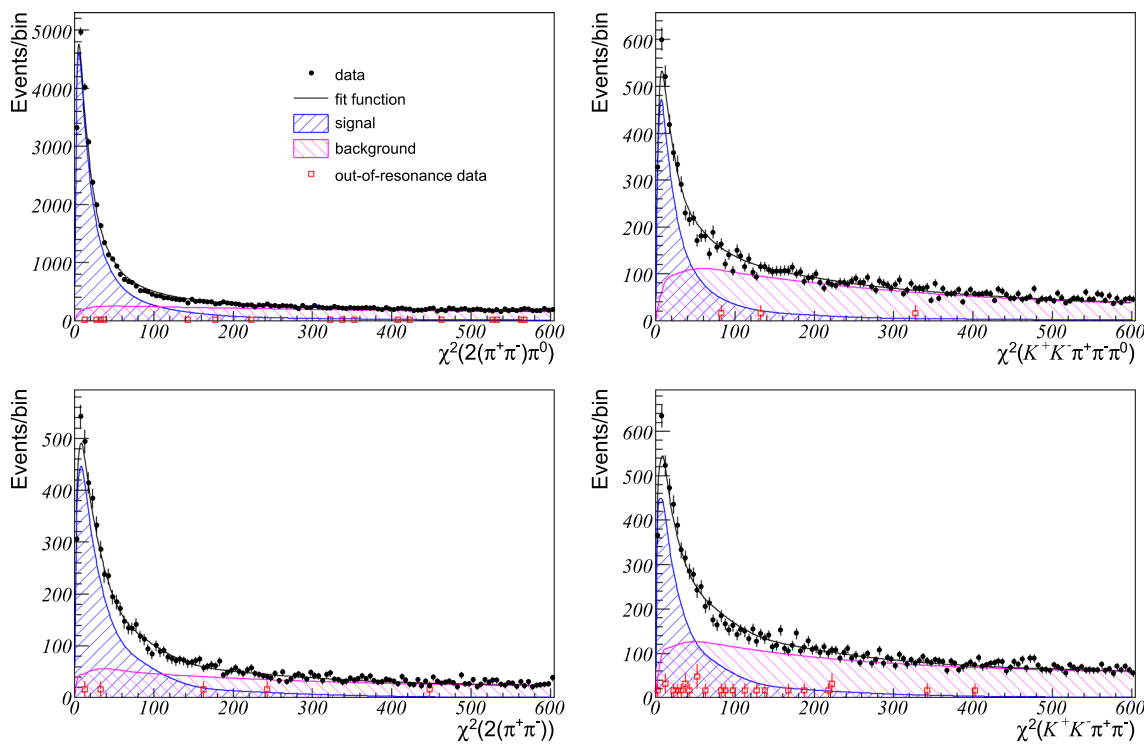


**Fig. 1** Distributions of  $\chi^2$  from kinematic fits for  $2(\pi^+\pi^-)\pi^0$ ,  $K^+K^-\pi^+\pi^-\pi^0$ ,  $2(\pi^+\pi^-)$  and  $K^+K^-\pi^+\pi^-$  selected candidate events. Black dots are experimental data collected at the  $J/\psi$  peak, red squares are data collected in the continuum and normalized as described in the

text. The black lines represent the results of fits using linear combinations of MC distributions for signal (blue hatched areas) and background (magenta hatched areas) decays of the  $J/\psi$

**Table 1** Numbers of selected signal events  $N_i^{peak}$  and  $N_i^{cont}$ , detection efficiencies  $\varepsilon_i$ , measured branching fractions  $B_i$  of  $J/\psi \rightarrow X_i$  decays and PDG data for these quantities. The given errors for detection effi-

ciencies  $\varepsilon_i$  are systematic, the first of the given errors for the measured branching fraction is statistical and the second one is systematic

	hadrons	$2(\pi^+\pi^-)\pi^0$	$K^+K^-\pi^+\pi^-\pi^0$	$2(\pi^+\pi^-)$	$K^+K^-\pi^+\pi^-$
$N_i^{peak}$	$4.62 \times 10^6$	22995	2616	2654	2671
$N_i^{cont}$	$32.3 \times 10^3$	4	0	8	2
$\varepsilon_i$ , %	93.8	$8.31 \pm 0.32$	$3.05 \pm 0.10$	$17.7 \pm 0.19$	$7.42 \pm 0.40$
$B_i$ , %	–	$5.44 \pm 0.07 \pm 0.33$	$1.74 \pm 0.08 \pm 0.24$	$0.288 \pm 0.014 \pm 0.024$	$0.704 \pm 0.026 \pm 0.092$
$B_i$ , % [1]	$87.7 \pm 0.5$	$3.73 \pm 0.32$	$1.20 \pm 0.30$	$0.357 \pm 0.030$	$0.686 \pm 0.028$

as  $2(\pi^+\pi^-)$  with an arbitrary number of additional photons were selected. It was also required that the condition  $E_{mis} > 0.4\text{GeV}$  be satisfied, where  $E_{mis} = M_{\psi} - \sum E_k$ ,  $M_{\psi}$  is the  $J/\psi$  mass, and the sum is taken over the energies of charged pions. The condition for  $E_{mis}$  was imposed to suppress the background from the  $J/\psi \rightarrow 2(\pi^+\pi^-)$  decays. For selected  $2(\pi^+\pi^-)\pi^0$  and  $2(\pi^+\pi^-)$  events, the distributions of the squared recoil mass of  $2(\pi^+\pi^-)$  system were considered. The experimental data were fitted using linear combinations of MC histograms for the  $J/\psi \rightarrow 2(\pi^+\pi^-)\pi^0$  decay and other  $J/\psi$  decays considered as background. In each range of the absolute value and polar angle of the recoil momentum of the  $2(\pi^+\pi^-)$  system, the background events

were subtracted and in this way the number  $N_5$  of the reconstructed  $\pi^0$  in the  $J/\psi \rightarrow 2(\pi^+\pi^-)\pi^0$  decays was determined from the selected  $2(\pi^+\pi^-)\pi^0$  events, and the number  $N_4$  of the  $\pi^0$  that were not reconstructed was determined from  $2(\pi^+\pi^-)$  events. In the same way  $N_5$  and  $N_4$  were determined in the simulation. The  $\pi^0$  registration efficiency was calculated as  $\varepsilon_{\pi^0} = N_5/(N_5 + N_4)$ , and for the experimental data it varies from 30 to 63%, depending on the angle and momentum of  $\pi^0$ . Later, when selecting events in a modeling for the determination of the detection efficiency in the  $J/\psi \rightarrow X_i$  decays, some of the selected events were discarded to make  $\varepsilon_{\pi^0}$  equal for data and simulation. The residual difference between the  $\pi^0$  registration efficiencies for

**Table 2** Summary of systematic uncertainties (in %) for the measured branching fractions of the decays  $J/\psi \rightarrow 2(\pi^+\pi^-)\pi^0$ ,  $J/\psi \rightarrow K^+K^-\pi^+\pi^-\pi^0$ ,  $J/\psi \rightarrow 2(\pi^+\pi^-)$  and  $J/\psi \rightarrow K^+K^-\pi^+\pi^-$ 

Source	$2(\pi^+\pi^-)\pi^0$	$K^+K^-\pi^+\pi^-\pi^0$	$2(\pi^+\pi^-)$	$K^+K^-\pi^+\pi^-$
$\chi^2$ distributions of the kinematic fits	1.0	3.9	3.6	2.9
Track registration efficiency	3.6	3.6	3.6	3.6
$\pi^0$ registration efficiency	1.5	1.5	—	—
Fake $\pi^0$	1.9	1.5	2.8	< 1
$\pi \rightarrow K$ misidentification	2.1	1.1	2.1	1.1
$K \rightarrow \pi$ misidentification	—	11.5	—	10.3
Fitting procedure	< 1	2.6	4.0	2.9
Threshold on $\chi^2$ of the kinematic fit	< 1	< 1	< 1	< 1
Trigger + selection cuts	< 1	< 1	< 1	< 1
Nonresonant background subtraction	1.6	1.6	1.6	1.6
Interference with the continuum	1.9	< 1	3.3	1.5
Angular and momentum distributions of final particles				
Helicity amplitudes of decay modes	1.6	1.9	1.1	2.2
Branching fractions of decay modes	2.0	2.9	< 1	4.9
Interference between decay mode amplitudes	< 1	< 1	< 1	< 1
Total	6.1	13.7	8.3	13.1

data and simulation was estimated and does not exceed 1.5% for all ranges of  $\pi^0$  angle and momentum.

With the above described selection criteria for signal events, there is a certain probability of appearing additional fake  $\pi^0$  in the event, which leads to the registration of the  $J/\psi \rightarrow X_i$  event as a background one. To assess the possible systematic error for the detection efficiency of signal events associated with this, for each  $J/\psi$  decay under study the probabilities of the presence of two additional photons for the selected signal events were compared for experimental data and modeling. Then, when simulating the  $J/\psi \rightarrow X_i$  decays, the fractions of events with an additional registered fake  $\pi^0$  for these channels were determined. Using these data, estimates were obtained for this systematic uncertainty, which are shown in Table 2.

The systematic error associated with the possible misidentification of charged pions as kaons was determined from the decays  $J/\psi \rightarrow \pi^+\pi^-\pi^0$ . For this, the experimental multihadron decays of  $J/\psi$  with two central tracks and one  $\pi^0$  were selected. For them, the values of  $\chi^2$  of the kinematic fit were determined under two hypotheses, assuming that the decay  $J/\psi \rightarrow \pi^+\pi^-\pi^0$  or  $J/\psi \rightarrow K^+K^-\pi^0$  took place, respectively. Then the events with the value of  $\chi^2$  under the first hypothesis less than half of the value under the second hypothesis were considered to originate from the  $J/\psi \rightarrow \pi^+\pi^-\pi^0$  decays. For them, in different ranges of track momenta, the fractions of tracks identified by the ToF or ATC systems as  $K^\pm$  were determined, from which the probabilities of misidentification  $P_{\pi \rightarrow K}$  were calculated. A small correction of 1–3% was made for possible

admixture of tracks originated from true  $K^\pm$  in the selected events, which was estimated using simulation. The probability  $P_{\pi \rightarrow K}$  determined in this way varies within 3–20%, depending on the momentum of the track. Later, when identifying tracks in the  $J/\psi \rightarrow X_i$  decays in the simulation, a correction was made in such a way as to reproduce the experimental probability  $P_{\pi \rightarrow K}$ . The systematic error associated with this correction when measuring the branching fractions of the  $J/\psi$  decays under study depends on accuracy of  $P_{\pi \rightarrow K}$  determination. It is small and does not exceed 2.1% for  $5\pi$  and  $4\pi$  decays, and 1.1% for  $2K3\pi$ ,  $2K2\pi$  decays, respectively.

The probability  $P_{K \rightarrow \pi}$  of misidentification of charged kaons as pions was determined from the experimental data, by decays  $\varphi \rightarrow K^+K^-$ . For this, the multihadron decays of  $J/\psi$  with two or four central tracks and zero total tracks charge were selected. It was also required that the event contains at least one pair of tracks identified as  $K^+K^-$ ,  $K^+\pi^-$  or  $K^-\pi^+$ . For these pairs, for different ranges of momenta of tracks in a pair, the pair mass distributions were considered under the assumption that both tracks were produced by kaons. The distributions clearly show the peaks from the  $\varphi \rightarrow K^+K^-$  decays, from which the numbers  $N_{KK}$  and  $N_{K\pi}$  of selected  $\varphi \rightarrow K^+K^-$  decays were determined for the  $KK$  and  $K\pi$  distributions, respectively. Then the kaon misidentification probability was calculated as  $P_{K \rightarrow \pi} = N_{K\pi}/(N_{KK} + N_{K\pi})$ . In the range of track momenta of 0.3–0.6 GeV/c, when kaon identification is made by the ToF system, it is equal 0.35–0.55. For track momenta in the range 0.6–1.0 GeV/c, with identification by the ATC system,

the probability of misidentification turns out to be equal 0.1–0.2. When identifying kaons in  $J/\psi \rightarrow X_i$  decays in the simulation, a correction was made to reproduce the  $P_{K \rightarrow \pi}$  probability obtained in the same way as for the data. The systematic errors associated with such a correction when determining the  $J/\psi \rightarrow X_i$  branching fractions for the final states  $2K3\pi$  and  $2K2\pi$  were calculated taking into account the angular and momentum distributions of the final particles in these decays. These errors are estimated to be 11.5% and 10.3%, respectively.

To estimate the systematic errors associated with the fitting procedure for the  $\chi^2$  distributions in Fig. 1, the fit ranges and bin widths of histograms varied. The resulting changes for the measured branching fractions of  $J/\psi \rightarrow X_i$  decays are given in Table 2. A twofold increase or decrease in the  $\chi^2$  threshold of the kinematic reconstruction for signal events gives a systematic error of less than 1%. It should also be noted that formula (1) for the decay branching fraction includes the ratio of the detection efficiencies of the decays under study and multihadron decays of  $J/\psi$ . As a result, the systematic errors associated with trigger requirements and multihadron events selection conditions are significantly reduced and also, according to estimates, do not exceed 1%.

The  $J/\psi$  decays under study can proceed through various intermediate states. In order to correctly determine the event detection efficiency for each decay channel, it is important to correctly specify the angular and momentum distributions of the final particles for all possible decay modes, as well as their relative probabilities in the simulation. For this, a generator based on the helicity formalism was used in the simulation. In the generator, the  $J/\psi$  decay for each mode was considered as proceeding through quasi-two-particle states. If intermediate state corresponds to some known resonance, then the dependence of helicity amplitude on the state mass was set as a Breit-Wigner one, with the values of the resonance parameters taken from the PDG. If this state does not have a resonance character, then the mass dependence was set as a constant. With such a choice of setting the amplitudes, they are defined up to arbitrary complex constants, and when determining the detection efficiency, a systematic error arises associated with the choice of specific values of the moduli and phases of these constants, which are usually unknown. To estimate this error, for each decay mode several dozen sets of constants were randomly generated and the detection efficiency was determined for each of them. Then the obtained mean efficiencies for modes were averaged over modes of the  $J/\psi \rightarrow X_i$  decay and the root-mean-square spread of the obtained mode-averaged efficiencies was considered as an estimate of the systematic error for this decay channel.

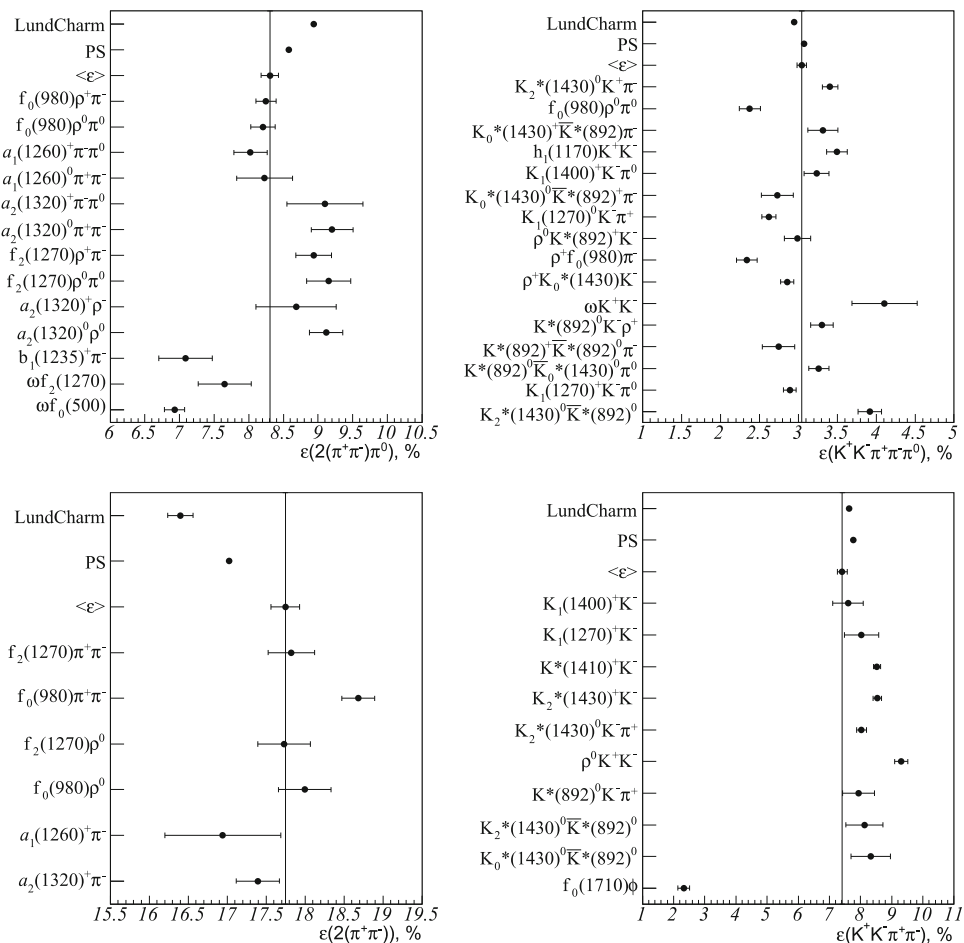
In Fig. 2 for each  $J/\psi \rightarrow X_i$  decay channel under study, the obtained mean detection efficiencies of the modes of this decay, which were modeled, are shown. The systematic errors associated with the uncertainties of the helicity amplitudes

are given as errors for the efficiencies. The mode-averaged detection efficiency  $\langle \varepsilon \rangle$  for each decay channel is also given. It was calculated as  $\langle \varepsilon \rangle = \sum \varepsilon_a B_a / \sum B_a$ , where  $\varepsilon_a$  is the detection efficiency for mode  $a$  and  $B_a$  is the branching fraction for this mode. The mode-averaged detection efficiency for the  $X_i$  channel was then used in formula (1) as the detection efficiency  $\varepsilon_i$ . The figure also shows the detection efficiencies determined by simulations using uniform phase space distributions for final particles (denoted as PS) as well as simulations with the LundCharm generator.

The branching ratios  $B_a$  for modes are known only for a small number of  $J/\psi$  decays. Therefore, to determine them, we considered the mass distributions for all combinations of final particles in a given  $J/\psi$  decay channel. The  $B_a$  values, considered as free parameters, were determined from the joint fit of these MC distributions to the experimental distributions. This method of determining the  $B_a$  values also leads to some systematic error for efficiency  $\langle \varepsilon \rangle$ , since these mass distributions in modeling depend, in general, on the set of helicity amplitudes used. In addition, for a given channel, there may be additional decay modes that were not taken into account in the simulation. To estimate this systematic uncertainty, many sets of branching ratios  $B_a^{(k)}$  were generated in such a way that for each mode  $a$  the quantities  $\log_2(B_a^{(k)}/B_a^{fit})$ , where  $B_a^{fit}$  is the branching ratio for mode  $a$ , obtained in the joint fit, obey the Gaussian distribution with mean 0 and standard deviation 1. For each set obtained, the mode-averaged detection efficiencies in the  $J/\psi \rightarrow X_i$  decay channel were determined. The root-mean-square spread of the obtained averaged efficiencies was considered as an estimate of the systematic error associated with uncertainties in  $B_a$  values for a given channel of decay. Systematic errors associated with the uncertainties of the helicity amplitudes, as well as branching ratios of decay modes, are given in Table 2.

The average detection efficiencies for the  $J/\psi \rightarrow X_i$  decays given in Table 1 were obtained under the assumption that there is no interference between the amplitudes of the decay modes. To estimate the systematic error associated with possible interference, an additional simulation was performed in which all decay modes for a given channel were generated simultaneously. In this case, the amplitude of the decay in the generator was set equal to the sum of the amplitudes of the modes, and the partial widths for the modes were set in accordance with the relative probabilities determined as described above. Several dozen sets of helicity amplitudes were generated, for each of them the detection efficiency was determined, and then the obtained efficiencies were averaged. Two possibilities were considered: in one case, the phases of the helicity amplitudes, like their moduli, were set randomly, and in another case, the relative phases were taken to be zero. For both cases, the difference in the average detection efficiency compared with the average detection efficiency

**Fig. 2** Detection efficiencies for different modes of  $J/\psi$  decays into the final states  $2(\pi^+\pi^-)\pi^0$ ,  $K^+K^-\pi^+\pi^-\pi^0$ ,  $2(\pi^+\pi^-)$  and  $K^+K^-\pi^+\pi^-\pi^0$ . Error bars show the systematic uncertainties associated with the uncertainties in the helicity amplitudes.  $\langle \varepsilon \rangle$  denotes the mode-averaged detection efficiency for a given final state. Also shown are the detection efficiencies determined from simulations using the uniform phase space distributions for final particles (denoted as PS) and from simulations using the LundCharm generator



obtained without taking into account the interference does not exceed 1%, i.e. the effects of interference between the amplitudes of the decay modes in determining the branching fractions of the decays under study can be neglected.

When subtracting the events of nonresonant background in formula (1), it is also necessary to estimate the magnitude of possible interference between amplitudes of the  $J/\psi \rightarrow X_i$  decay under study and nonresonant  $e^+e^- \rightarrow X_i$  processes. The values of these contributions can change noticeable depending on what are the phases of the individual decay modes relative to the continuum process phase, as well as on the ratios of their partial widths to each other. Recently, the BES collaboration measured [8] relative phase between the strong and electromagnetic amplitudes of the decay  $J/\psi \rightarrow 2(\pi^+\pi^-)\pi^0$ , assuming 100% interference between them. The found relative phase turned out to be close to  $\pm 90^\circ$ , which may indicate that the phases of the amplitudes of individual decay modes relative to the phase of the continuum are the same. Taking this circumstance into account, the estimates of the systematic error associated with possible interference with the continuum were made in our work under the assumption of the maximum possible interference. To do this, first, using formulas from work [19], we calculated the cross sections for the processes  $e^+e^- \rightarrow J/\psi \rightarrow \text{hadrons}$

and  $e^+e^- \rightarrow J/\psi \rightarrow X_i$ , while the center-of-mass energy spread was set equal to  $\sigma_W = 0.7$  MeV, and the interference with the continuum was not taken into account. Then, from the numbers of signal events (Table 1) at the  $J/\psi$  peak and for off-resonance data, the ratios of the cross sections at the peak and in the continuum for the processes  $e^+e^- \rightarrow \text{hadrons}$  and  $e^+e^- \rightarrow X_i$  were estimated. For the  $e^+e^- \rightarrow \text{hadrons}$  process, the cross section in the continuum was evaluated from the  $e^+e^- \rightarrow \mu^+\mu^-$  cross section [8], for the  $e^+e^- \rightarrow 2(\pi^+\pi^-)\pi^0$  process, the cross section was also taken from this paper. After that, for each  $J/\psi \rightarrow X_i$  decay, the maximum possible change in the cross section at the  $J/\psi$  peak was calculated taking into account the interference between  $J/\psi$  and the continuum, for what the relative phase of the interference was set equal to  $\varphi = 90^\circ$ . For  $2(\pi^+\pi^-)$  channel interference was not taken into account, since, due to non-conservation of  $G$ -parity in this channel, the decay  $J/\psi \rightarrow 2(\pi^+\pi^-)$  can only proceed through a photon. The results of calculations are shown in Table 3. Shown are the cross sections for the processes  $e^+e^- \rightarrow J/\psi \rightarrow \text{hadrons}$ ,  $e^+e^- \rightarrow J/\psi \rightarrow X_i$  at the  $J/\psi$ -meson peak energy, the ratios of the cross sections in the continuum and at the  $J/\psi$  peak, as well as the maximum possible change in the cross section at the  $J/\psi$  peak

**Table 3** Cross sections for the processes  $e^+e^- \rightarrow J/\psi \rightarrow$  hadrons,  $e^+e^- \rightarrow J/\psi \rightarrow X_i$  at the  $J/\psi$  peak and the maximum possible change in the cross section at the  $J/\psi$  peak with interference taken into account

	$\sigma_{J/\psi, \text{nb}}$	3774	215	73.2	13.3
$\sigma_{\text{cont}}/\sigma_{J/\psi, \text{nb}}, \%$	0.6	0.1	$0^{+0.6}$	$4.8 \pm 1.7$	$1.2 \pm 0.9$
$\Delta\sigma_{\text{max}} (\varphi=90\%), \%$	3.3	1.4	3.4	$< 1$	4.8
$e^+e^- \rightarrow J/\psi \rightarrow$ hadrons					
$e^+e^- \rightarrow J/\psi \rightarrow 2(\pi^+\pi^-)\pi^0$				$e^+e^- \rightarrow J/\psi \rightarrow K^+\pi^+\pi^-\pi^0$	$e^+e^- \rightarrow J/\psi \rightarrow 2(\pi^+\pi^-)$
$e^+e^- \rightarrow J/\psi \rightarrow X_i$				$e^+e^- \rightarrow J/\psi \rightarrow K^+\pi^+\pi^-\pi^0$	$e^+e^- \rightarrow J/\psi \rightarrow K^+K^-\pi^+\pi^-$

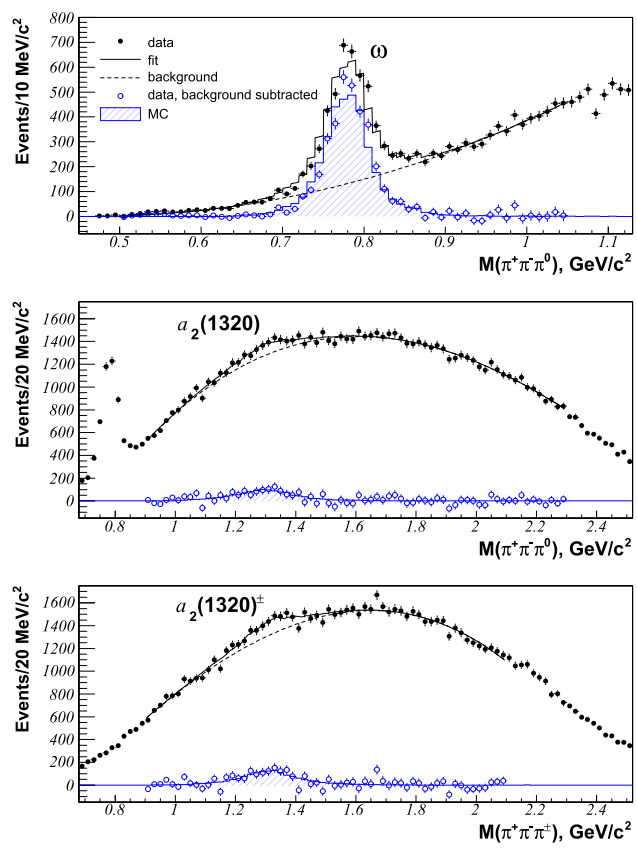


**Fig. 3** Masses of  $\pi^+\pi^-\pi^0$  and  $\pi^+\pi^-\pi^\pm$  in selected signal events of  $J/\psi \rightarrow 2(\pi^+\pi^-)\pi^0$  decays (all combinations per event are shown). Close circles are experimental data, black solid lines are the sums of MC histograms for the corresponding decays through resonances (hatched histograms) and backgrounds (dashed lines), open circles are the data after subtracting backgrounds

when taking into account the interference. The systematic uncertainties for the branching fractions of the  $J/\psi \rightarrow X_i$  decays under study, associated with possible interference with the continuum, shown in Table 2, were obtained under the assumption of correlated variations for the numbers of selected signal events of  $J/\psi \rightarrow$  hadrons and  $J/\psi \rightarrow X_i$  decays.

#### 4 $J/\psi$ decays involving intermediate resonance

Considering the mass distributions of systems of final particles for signal events of  $J/\psi \rightarrow X_i$  decays, we also estimated the branching fractions of some  $J/\psi$  decays involving intermediate resonances. Figures 3, 4 and 5 show such mass distributions, which were used to determine branching fractions of decays through  $a_2$ ,  $\rho$ ,  $\omega$ ,  $K^*$  and  $K_2^*$  mesons. The distributions were fitted using linear combinations of the MC distributions for the events of the corresponding decays and backgrounds, specified as polynomials.

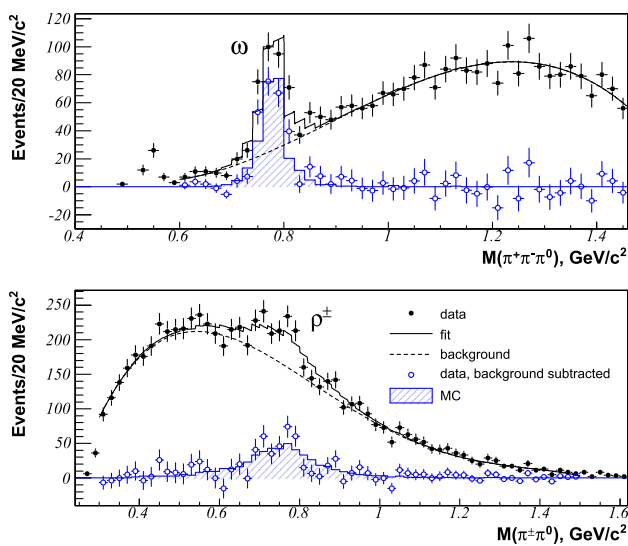


**Fig. 4** Masses of  $\pi^+\pi^-\pi^0$  and  $\pi^\pm\pi^0$  in selected signal events of  $J/\psi \rightarrow K^+K^-\pi^+\pi^-\pi^0$  decays. Close circles are experimental data, black solid lines are the sums of MC histograms for the corresponding decays through resonances (hatched histograms) and backgrounds (dashed lines), open circles are the data after subtracting backgrounds

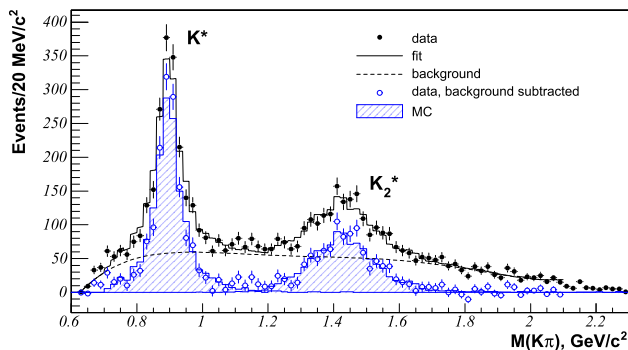


**Fig. 5** Masses of  $K^+\pi^-$  and  $K^-\pi^+$  in selected signal events of  $J/\psi \rightarrow K^+K^-\pi^+\pi^-$  decays. Close circles are experimental data, black solid lines are the sums of MC histograms for the corresponding decays through resonances (hatched histograms) and backgrounds (dashed lines), open circles are the data after subtracting backgrounds

The branching fraction  $B_R$  of decay through resonance  $R$  was calculated using the formula

$$B_R = B_i \frac{N_R^{\text{peak}} \varepsilon_i^{\text{MC}}}{N_i^{\text{peak}} \varepsilon_R^{\text{MC}}}, \quad (2)$$

where  $B_i$  is the previously measured branching fraction of the  $J/\psi \rightarrow X_i$  decay,  $N_R^{\text{peak}}$  is the number of selected signal events for decays through the resonance, determined from

the fit,  $\varepsilon_R^{\text{MC}}$  is the detection efficiency for decay through resonance, determined from simulation.

Table 4 shows the results for measured branching ratios of  $J/\psi$  decays involving intermediate resonances. The detection efficiencies for the corresponding decays, the numbers of signal events, the measured branching fractions, as well as the results of measurements performed by other groups, are given. The efficiencies  $\varepsilon_R^{\text{MC}}$  were determined similarly to the detection efficiencies for decay modes, as weighted averages over the detection efficiencies of modes contributing to a given decay. In the table, for  $\varepsilon_R^{\text{MC}}$  the systematic error of determination is shown, for  $N_R^{\text{peak}}$  and  $B_R$  the first of the given errors is statistical, the second is systematic.

To estimate the systematic uncertainties for  $N_R^{\text{peak}}$ , we varied the ranges of fits of the distributions in Figs. 3, 4 and 5, histogram bin widths and the orders of the background polynomials. Also, estimates were made of the systematic uncertainty associated with possible interference of the amplitude of decay through an intermediate resonance with the amplitudes of decays through other resonances with the same spin and parity. For this, in addition to the decay modes, shown in Fig. 2, the decays through  $a_2(1700)$ ,  $\rho(1450)$ , and  $K_2^*(1980)$  resonances were also modeled. The obtained branching fractions of decays through resonances were compared for two cases, with and without interference. The interference effects were taken into account in the same way as described above when determining systematic errors for the  $J/\psi \rightarrow X_i$  decays probabilities. The total systematic uncertainty for  $B_R$  was calculated taking into account the systematic errors for the corresponding  $J/\psi \rightarrow X_i$  decay channel, determined earlier and shown in Table 2, the error for  $N_R^{\text{peak}}$ , and the uncertainties associated with interference.

Using the measured branching fraction of the decay  $J/\psi \rightarrow \omega\pi^+\pi^- \rightarrow 2(\pi^+\pi^-)\pi^0$  and the PDG value of branching fraction for the decay  $\omega \rightarrow \pi^+\pi^-\pi^0$ , which is  $(89.2 \pm 0.7)\%$  [1], we have obtained the value of the branching fraction of the decay  $J/\psi \rightarrow \omega\pi^+\pi^-$ , given in Table 4, which is in good agreement with the BABAR result [6, 7]. Calculated in a similar way, our value for the  $J/\psi \rightarrow \omega K^+K^-$  decay probability turns out to be noticeably higher than the values obtained by the DM2 [20] and BABAR [6, 7] groups. In the same way, taking the value 2/3 for the probability of the  $K^*(892)^0 \rightarrow K^+\pi^-$  decay, the branching fraction for the  $J/\psi \rightarrow K^*(892)^0 K^-\pi^+ + \text{c.c.}$  decay is obtained, given in Table 4, which is in agreement with the PDG value, but has nearly twice the accuracy.

**Table 4** Measured or calculated branching fractions  $B_R$  of  $J/\psi$  decays involving intermediate resonances. The given errors for detection efficiencies  $\varepsilon_R$  are systematic, the first of the given errors for the number of selected signal events  $N_R^{peak}$  is statistical and the second one is systematic

Decay	$\varepsilon_R^{MC}$ , %	$N_R^{peak}$	Branching fraction $B_R$ , %	Previous works
			This work	
$J/\psi \rightarrow a_2(1320)^0 \pi^+ \pi^- \rightarrow 2(\pi^+ \pi^-) \pi^0$	9.12 ± 0.29	1317 ± 36 ± 265	0.284 ± 0.008 ± 0.060	–
$J/\psi \rightarrow a_2(1320)^+ \pi^- \pi^0 + \text{c.c.} \rightarrow 2(\pi^+ \pi^-) \pi^0$	8.71 ± 0.56	1628 ± 40 ± 247	0.367 ± 0.009 ± 0.073	–
$J/\psi \rightarrow \omega \pi^+ \pi^- \rightarrow 2(\pi^+ \pi^-) \pi^0$	7.34 ± 0.27	3531 ± 59 ± 212	0.946 ± 0.016 ± 0.108	–
$J/\psi \rightarrow \omega \pi^+ \pi^-$	–	–	1.06 ± 0.02 ± 0.12	0.72 ± 0.10 [1], 0.97 ± 0.09 [6,7]
$J/\psi \rightarrow \omega K^+ K^- \rightarrow K^+ K^- \pi^+ \pi^- \pi^0$	4.11 ± 0.42	276 ± 17 ± 17	0.136 ± 0.008 ± 0.026	–
$J/\psi \rightarrow \omega K^+ K^-$	–	–	0.153 ± 0.009 ± 0.029	0.074 ± 0.024 [20], 0.067 ± 0.026 [6,7]
$J/\psi \rightarrow \rho^+ K^+ K^- \pi^- + \text{c.c.} \rightarrow K^+ K^- \pi^+ \pi^- \pi^0$	2.79 ± 0.063	485 ± 22 ± 94	0.353 ± 0.016 ± 0.081	–
$J/\psi \rightarrow K^*(892)^0 K^- \pi^+ + \text{c.c.} \rightarrow K^+ K^- \pi^+ \pi^-$	8.00 ± 0.39	1559 ± 39 ± 17	0.381 ± 0.010 ± 0.054	–
$J/\psi \rightarrow K^*(892)^0 K^- \pi^+ + \text{c.c.}$	–	–	0.573 ± 0.014 ± 0.082	0.77 ± 0.16 [1]
$J/\psi \rightarrow K_2^*(1430)^0 K^- \pi^+ + \text{c.c.} \rightarrow K^+ K^- \pi^+ \pi^-$	8.06 ± 0.23	1094 ± 33 ± 90	0.265 ± 0.080 ± 0.044	–

**Acknowledgements** The authors are grateful to V.P. Druzhinin and E.P. Solodov for useful discussions. This work was supported by the Ministry of Education and Science of the Russian Federation, RFBR Grant 16-02-00392-a and RF Presidential Grant for Sc. Sch. NSh-2479.2014.2.

**Data Availability Statement** This manuscript has no associated data or the data will not be deposited. [Authors' comment: The data that support the findings of this study are available from the corresponding author upon reasonable request.]

**Open Access** This article is licensed under a Creative Commons Attribution 4.0 International License, which permits use, sharing, adaptation, distribution and reproduction in any medium or format, as long as you give appropriate credit to the original author(s) and the source, provide a link to the Creative Commons licence, and indicate if changes were made. The images or other third party material in this article are included in the article's Creative Commons licence, unless indicated otherwise in a credit line to the material. If material is not included in the article's Creative Commons licence and your intended use is not permitted by statutory regulation or exceeds the permitted use, you will need to obtain permission directly from the copyright holder. To view a copy of this licence, visit <http://creativecommons.org/licenses/by/4.0/>.

Funded by SCOAP<sup>3</sup>. SCOAP<sup>3</sup> supports the goals of the International Year of Basic Sciences for Sustainable Development.

## References

1. P.A. Zyla et al., (Particle Data Group), *Prog. Theor. Exp. Phys.* **2020**, 083C01 (2020)
2. B. Jean-Marie et al., Determination of the G parity and isospin of  $\psi(3095)$  by study of multipion decays. *Phys. Rev. Lett.* **36**, 29 (1976)
3. J. Burmester et al., PLUTO Collaboration, Decays  $J/\psi(3.1) \rightarrow f\omega$  and  $J/\psi(3.1) \rightarrow B\pi$ . *Phys. Lett. B* **72**, 135 (1977)
4. M.E.B. Franklin et al., Measurement of  $\psi(3097)$  and  $\psi(3686)$  decays into selected hadronic modes. *Phys. Rev. Lett.* **51**, 963 (1983)
5. J.E. Augustin et al., DM2 Collaboration, Study of the  $J/\psi$  decay into five pions. *Nucl. Phys. B* **320**, 1 (1989)
6. B. Aubert et al., BABAR Collaboration, The  $e^+e^- \rightarrow 2(\pi^+\pi^-)\pi^0$ ,  $2(\pi^+\pi^-)\eta$ ,  $K^+K^-\pi^+\pi^-\pi^0$  and  $K^+K^-\pi^+\pi^-\eta$  cross sections measured with initial-state radiation. *Phys. Rev. D* **76**, 092005 (2007)
7. B. Aubert, et al., BABAR Collaboration, The  $e^+e^- \rightarrow 2(\pi^+\pi^-)\pi^0$ ,  $2(\pi^+\pi^-)\eta$ ,  $K^+K^-\pi^+\pi^-\pi^0$  and  $K^+K^-\pi^+\pi^-\eta$  cross sections measured with initial-state radiation. *Phys. Rev. D* **77**, 119902 (2008) (**Erratum**)
8. M. Ablikim et al., BESIII Collaboration, Measurement of the phase between strong and electromagnetic amplitudes of  $J/\psi$  decays. *Phys. Lett. B* **791**, 375 (2019)
9. J.P. Lees et al., BABAR Collaboration, Study of reactions  $e^+e^- \rightarrow 2(\pi^+\pi^-)\pi^0\pi^0\pi^0$  and  $2(\pi^+\pi^-)\pi^0\pi^0\eta$ , at center-of-mass energies from threshold to 4.5 GeV using initial-state radiation. *Phys. Rev. D* **103**, 092001 (2021)
10. F. Vannucci et al., Mesonic decays of the  $\psi(3095)$ . *Phys. Rev. D* **15**, 1814 (1977)
11. V.V. Anashin et al., KEDR Collaboration, The KEDR detector. *Phys. Part. Nucl.* **44**, 657 (2013)
12. V.V. Anashin, et al., in: 6th European Particle Accelerator Conference, EPAC 98, Stockholm, Sweden, 22–26 June (1998), p. 400
13. R. Brun et al., GEANT 3.21, CERN Program Library Long Writeup W5013, (1993). <https://rampex.ihep.su/manuals/geant321.pdf>

14. M. Jacob, G.C. Wick, On the general theory of collisions for particles with spin. *Ann. Phys.* **281**, 774 (2000)
15. J.D. Richman, An experimenter's guide to the helicity formalism, CALT-68-1148. <https://inspirehep.net/literature/202987>
16. J.C. Chen et al., Event generator for  $J/\psi$  and  $\psi(2S)$  decay. *Phys. Rev. D* **62**, 034003 (2000)
17. T. Sjostrand, M. Bergson, The Lund Monte Carlo for jet fragmentation and  $e^+e^-$  physics-jetset version 6.3: an update. *Comput. Phys. Commun.* **43**, 367 (1987)
18. E. Barberio, Z. Was, PHOTOS: a universal Monte Carlo for QED radiative corrections: version 2.0, CERN-TH.7033/93
19. K.Y. Todyshev, The application Breit–Wigner form with radiative corrections to the resonance fitting. [arXiv:0902.4100v3](https://arxiv.org/abs/0902.4100v3)
20. A. Falvard et al., Study of hadronic  $J/\psi$  decays involving  $\varphi$  and  $\omega$  production. *Phys. Rev. D* **38**, 2706 (1988)